

Diffusion spectrum imaging predicts hippocampal sclerosis in mesial temporal lobe epilepsy patients

Zhen-Ming Wang^{1,2}, Peng-Hu Wei³, Miao Zhang^{1,2}, Chunxue Wu^{1,2}, Yi Shan^{1,2}, Fang-Cheng Yeh⁴, Yongzhi Shan³ & Jie Lu^{1,2} 

¹Department of Radiology and Nuclear Medicine, Xuanwu Hospital, Capital Medical University, Beijing, China

²Beijing Key Laboratory of Magnetic Resonance Imaging and Brain Informatics, Beijing, China

³Department of Neurosurgery, Xuanwu Hospital, Capital Medical University, Beijing, China

⁴Department of Neurological Surgery, University of Pittsburgh School of Medicine, Pittsburgh, Pennsylvania, USA

Correspondence

Jie Lu, Department of Radiology and Nuclear Medicine, Xuanwu Hospital, Capital Medical University, No. 45 Changchun Street, Xicheng District, Beijing, 100053, China.
Tel: +86-010-83198379; Fax: +86-010-83198379; E-mail: imaginglu@hotmail.com

Funding information

This project was supported by Beijing Municipal Administration of Hospitals' Ascent Plan (DFL20180802), the National Natural Science Foundation of China (grant numbers 81871009, 81801288, 82030037, 81790652), Huizhi Ascent Project of Xuanwu Hospital (HZ2021ZCLJ005), and Beijing Hospitals Authority Youth Program (QML20190805). Data were provided in part by the Human Connectome Project, WU-Minn Consortium (Principal Investigators: David Van Essen and Kamil Ugurbil; 1U54MH091657) funded by the 16 NIH Institutes and Centers that support the NIH Blueprint for Neuroscience Research; and by the McDonnell Center for Systems Neuroscience at Washington University.

Received: 1 November 2021; Revised: 20 December 2021; Accepted: 28 December 2021

Annals of Clinical and Translational Neurology 2022; 9(3): 242–252

doi: 10.1002/acn3.51503

Introduction

Epilepsy is one of the most common neurological disorders worldwide.^{1,2} Although epilepsy causes aberrant electrical discharges, it is molecularly associated with abnormal local gamma-aminobutyric acid/glutamatergic neuronal activity.³ Malfunction of microscale networks,

Abstract

Objectives: Epileptic patients suffer from seizure recurrence after surgery due to the challenging localization. Improvement of the noninvasive imaging-based approach for a better definition of the abnormalities would be helpful for a better outcome. **Methods:** The quantitative anisotropy (QA) of diffusion spectrum imaging (DSI) is a quantitative scalar of evaluating the water diffusivity. Herein, we investigated the association between neuronal diameters or density acquired in literature and QA of DSI as well as the seizure localization in temporal lobe epilepsy. Thirty healthy controls (HCs) and 30 patients with hippocampal sclerosis (HS) were retrospectively analyzed. QA values were calculated and interactively compared between the areas with different neuronal diameter/density acquired from literature in the HCP-1021 template. Diagnostic tests were performed on Z-transformed asymmetry indices (AIs) of QA (which exclude physical asymmetry) among HS patients to evaluate its clinical value. **Results:** The QA values in HCs conformed with different pyramidal cell distributions ranged from giant to small; corresponding groups were the motor-sensory, associative, and limbic groups, respectively. Additionally, the QA value was correlated with the neuronal diameter/density in cortical layer IIIc (correlation coefficient with diameter: 0.529, $p = 0.035$; density: -0.678 , $p = 0.011$). Decreases in cingulum hippocampal segments (Chs) were consistently observed on the sclerosed side in patients. The area under the curve of the Z-transformed AI in Chs to the lateralization of HS was 0.957 (sensitivity: 0.909, specificity: 0.895). **Interpretation:** QA based on DSI is likely to be useful to provide information to reflect the neuronal diameter/density and further facilitate localization of epileptic tissues.

such as neuron-glia interaction networks,⁴ plays a vital role in the process of seizure priming³; however, these microscale gray matter abnormalities are often challenging to detect in humans. Localizing the epileptogenic focus is challenging during presurgical evaluation; even experts at best achieve 50% accuracy if only routine magnetic resonance images (MRI) are used as references.⁵ Thus,

approaches that can evaluate the gray matter components are needed.

Diffusion tensor imaging can evaluate water molecule diffusion anisotropy in the living brain and has been used to evaluate epileptic connectomes.⁶ It has also been introduced to investigate microanatomic properties in epileptic disease⁷; The human neocortex comprises six laminae,^{8–11} with pyramidal, granule, and fusiform cells distributed among these layers; specifically, layer III and layer V were named as external and internal pyramidal layers.^{12–14} Laminar components differ between subregions; in particular, the majority of white matter comprises pyramidal cell (PC) axons. Giant PCs, primarily distributed among the Rolandic areas and visual and acoustic cortices, are neurons that typically conduct faster, project over longer distances, and are involved with primary function. Smaller PCs, mainly located in the frontal lobe and temporo-parieto-occipital areas, conduct slower and primarily deal with higher brain functions. Hippocampal PCs have also been comprehensively explored; notably, their neuronal diameter is greater on the left side.¹⁵ PCs account for 75% and 80% of the total gray matter neurons and white matter is mainly composed of PC axons¹⁶; hence, determining the components or abnormalities of the gray matter by quantifying the properties of white matter may be feasible. This might be of clinical value, especially for diseases such as hippocampal sclerosis (HS), which includes PC losses.¹⁷

However, DTI only assesses the average fiber orientation in a voxel. Diffusion spectrum imaging (DSI) is a recently developed approach that acquires enormous white matter diffusion directions within a voxel. Quantitative anisotropy (QA) derived from DSI can quantify complex distributions of intravoxel directions; therefore, DSI may be valuable in the assessment of tissue properties.¹⁸ Temporal lobe epilepsy (TLE) is the most common type of epilepsy. TLE 30%–40% of the patients are MRI negative, while approximately 15%–20% of the patients still have residual seizures.¹⁹ Therefore, identifying the tissue properties of TLE for a better localization might be of great value for clinical practice. In our previous study of small sample data, we got a preliminary impression that temporal local QA is beneficial for seizure localization.²⁰ In this study, we first evaluated the accuracy of the DSI QA revealing the tissue properties with comparison to cellular data from previous studies,^{12,21} then we quantified the efficiency of the DSI QA in lateralizing the epileptogenesis in patients with TLE.

Materials and Methods

This retrospective study included 30 healthy controls (HCs) and 30 mesial TLE patients with unilateral HS (19

left, 11 right) enrolled between October 2019 and January 2021 at our radiological department; detailed clinical data are shown in Table 1 and Table S1. The healthy volunteers were enrolled from the university campus and evaluated by two experienced radiologists and two neurologists to make sure that there were no neurological or mental disorders. Two experienced neuroradiologists evaluated the basic MRI images of the 30 patients with HS enrolled in this study. Specifically, 22 of these patients' basic MRIs showed reduced hippocampal volume and increased signal intensity on the ipsilateral side with T2 FLAIR images, while the other eight patients were MRI negative and hard to diagnose using only basic MRI. Written informed consent was obtained from all participants, and the institution's ethical committee approved the study.

To observe the differences in extracted QA values across groups with different pyramidal diameters and functions, we first classified the subcortical regions of the JHU White Matter Labels (1 mm) atlas in local HCs into groups of motor/sensory, associative, and limbic fibers. The neuronal diameter/density information in literature^{12,21} and QA of different regions in the HCP-1021 template (<https://pitt.box.com/v/HCP1021-1mm>) were analyzed to investigate the association in normal brain tissues.

Patients with HS were enrolled, and the epileptogenic foci of these patients was localized via pathological findings or seizure freedom after treatment. The QA scalars of the hippocampus were quantified using comprehensive statistics to evaluate the global QA changes in HS patients, and further forecast value to the HS lateralization was observed. The flow diagram of the procedure is shown in Figure 1.

Image acquisition

DSI results were acquired using a SIGNA Premier 3.0 Tesla MRI scanner (GE Healthcare, Milwaukee, WI, USA) with a

Table 1. Demographic features of the population.

Variable	HS (<i>n</i> = 30)	HC (<i>n</i> = 30)	<i>p</i> -value
Sex (M/F)	16/14	13/17	0.438
Age (y)	29.6 (14–53)	24.6 (19–33)	0.054
Age at epilepsy onset (y)	16.6 (1–38)	—	—
Epilepsy duration (y)	12.9 (1–30)	—	—
Monthly seizure frequency (times/month)	>15, <i>n</i> = 5; 6–15, <i>n</i> = 5; 3–5, <i>n</i> = 5; 1–3, <i>n</i> = 15	—	—
HS laterality	Left, <i>n</i> = 19; Right, <i>n</i> = 11	—	—

Abbreviations: HC, healthy controls; HS, hippocampal sclerosis.

Quantitative continuous variables: Mean, with range in parentheses.

64-channel phased-array coil. The parameters were as follows: echo time (TE) = 84.2 msec, repetition time (TR) = 5589 msec, field of view = 224 mm × 224 mm, voxel size = 2 × 2 × 2 mm³, maximum *b*-value = 7000 sec/mm², total diffusion directions = 257, in-plane resolution = 2 mm, and slice thickness = 2 mm. T1 anatomical reference images were acquired using high-resolution T1-weighted magnetization-prepared rapid acquisition gradient-echo sequences (TE = 2.69 msec, TR = 2477 msec, flip angle = 8°, isotropic 1.0-mm voxels).

DSI data analysis

We first reconstructed the spin distribution function¹⁸ in all individual spaces using DSI Studio software (<http://dsi-studio.labsolver.org>). The diffusion data were reconstructed using generalized q-sampling imaging¹⁸ as previously described.²²

ROI-based global quantification of QA values

Whole-brain level QA values were extracted, and the JHU White Matter Labels (1 mm) atlas was used to parcel the global white matter into 48 ROIs. The mean QA value of each ROI was calculated using MATLAB (MathWorks, Natick, MA, USA). Then, we compared the individual QA values of different white matter ROIs in the HS patients with the HCs, to determine if the presence of white matters with low QA values outside the temporal lobe was related to worse seizure outcomes.

Functional criteria for ROI classification

ROIs containing motor, sensory, auditory, or visual fibers were parcellated into the motor/sensory (including fibers associated with primary and secondary cortices) group according to function,²³ and these contained giant PC

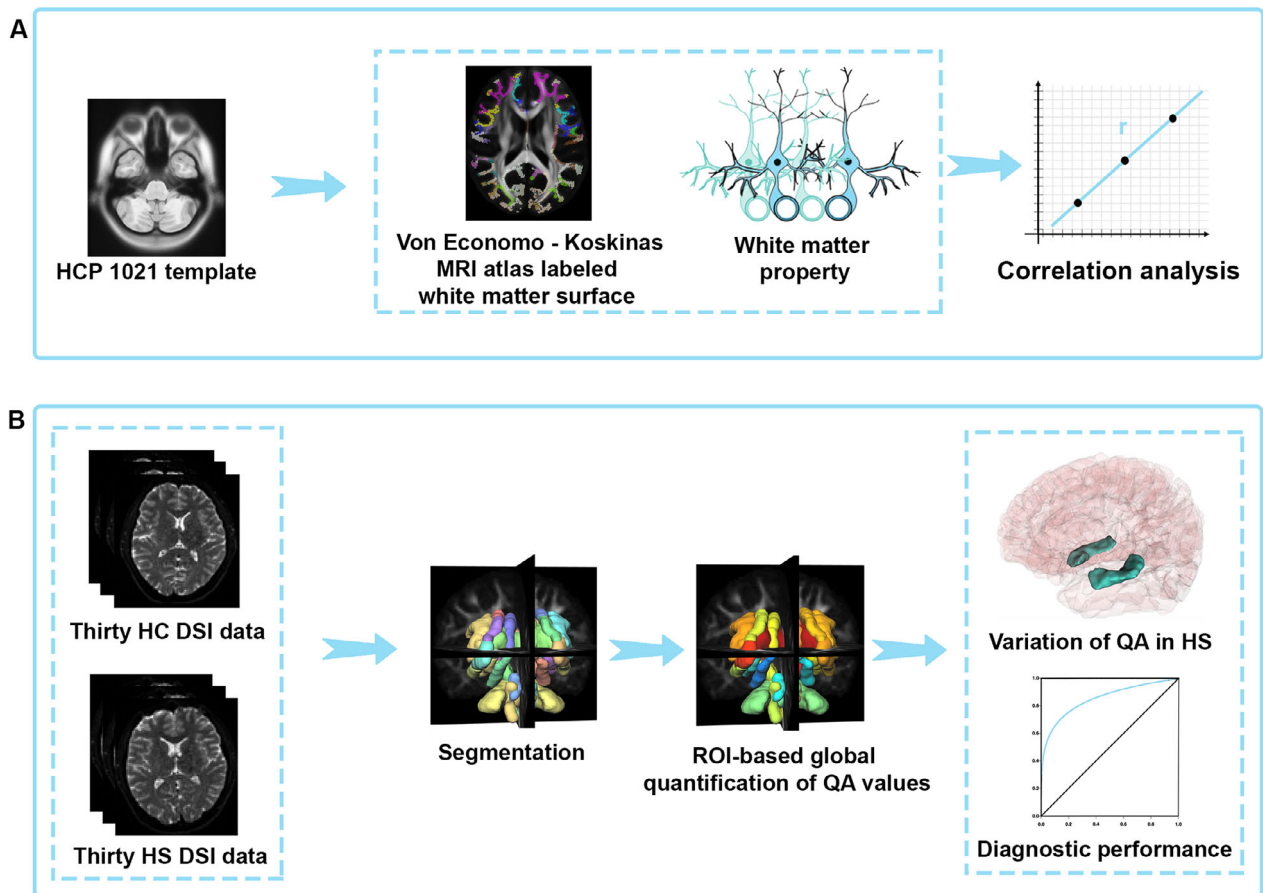


Figure 1. Flow diagram. (A) In the HCP-1021 template, the QA values at the insertion of the subcortical white matter were compared with neuronal diameter/density of the covering gray matter to observe their correlative relationship. (B) Thirty healthy participants and 30 HS patients were enrolled. The JHU White Matter Labels (1 mm) atlas were used for segmentation. The mean QA value of each white matter ROI was subsequently extracted. Finally, statistical analyses were performed, including the variation of QA values in HS patients and diagnostic performance of QA value. HC, healthy controls, HS, hippocampal sclerosis, QA, quantitative anisotropy; ROI, region of interest.

fibers.¹² In contrast, the ROIs carrying fibers to the dorsal prefrontal cortices, new cortical regions of the anterior temporal lobe, and speech-related fibers were classified into the associative group; these contained small PC fibers. The limbic group included all segments of the cingulum and fornix body (Table 2).²⁴

Descriptive statistical analyses were performed to determine the global QA value differences between the motor-sensory, associative, and limbic groups and the hippocampus-related fibers. The significance ($p < 0.05$) of these differences was determined using SPSS (Statistical Package for the Social Sciences version 23; IBM, Armonk, NY, USA).

Relationship between QA values and the Von Economo-Koskinas atlas

We generated a QA map with the HCP-1021 template to obtain an average QA distribution across a large population and labeled it with the Von Economo-Koskinas atlas. The atlas contains detailed cell diameters and density of different layers concerning different brain subregions.¹² An MRI version of the atlas became available recently.²¹ With FreeSurfer software (<https://surfer.nmr.mgh.harvard.edu/fswiki/DownloadAndInstall>), we strictly defined the ROI of brain regions to the insertion of subcortical white matter to extract the mean QA value of different areas in the QA map of the HCP-1021 average template, thereby facilitating a quantified analysis between the QA and cellular parameters. The average values of cell diameters and density (Tables S2 and S3) and the laminar thicknesses of layers I, II, IIIa, IIIb, IIIc, IV, Va, Vb, VIa, and VIb (these layers or sub-layer have relatively articulate neuronal diameter/density records) were compared with the mean QA values by Spearman correlation analysis in a region-by-region manner.

Patients' diagnostic test

Thirty patients with HS were enrolled to evaluate the QA in pathological brain tissues. We first plotted the violin plot of patients. Subsequently, we calculated the asymmetry index (AI) of QA value in ROIs and the mean and standard deviation in HCs. AI was defined as follows:

$$AI = (L - R) / (L + R)$$

where L and R represents the fiber tract QA value on the left and right side, respectively. As the distribution of diffusion scalars among different tracts was reported to be asymmetrical in healthy people,^{25,26} Z-transformation was performed on the AIs of patients using the mean \pm standard deviation in the previous step. To determine the diagnostic value of these Z-scores during HS

Table 2. Fiber classification according to function in literature.

Groups	Fibers	Connections
MSG	Body of corpus callosum	Connecting bilateral Rolandic areas
MSG	Cerebral peduncle	Containing M1 and M2 fibers
MSG	Posterior limb of internal capsule	Containing motor and sensory fibers
MSG	Optic radiation	Optic pathway
MSG	Retrolenticular part of internal capsule	Carrying the optic radiation
MSG	Splenium of corpus callosum	Connecting bilateral optic centrals
MSG	Superior corona radiata	Carrying pyT fibers
AG	Anterior corona radiata	Carrying fibers to anterior frontal lobe
AG	Anterior limb of internal capsule	Carrying fibers to anterior frontal lobe
AG	Genu of corpus callosum	Connecting bilateral anterior frontal lobe
AG	Posterior corona radiata	Containing parietal fibers
AG	Sagittal stratum	Containing inferior fronto-occipital fasciculus fibers dealing with semantic processing
AG	Superior longitudinal fasciculus	Associated with speaking, tool use, perspective taking, and empathy
AG	Tapetum	The tapetum curves anteriorly into the temporal lobe, extending almost to the tip of the temporal horn just lateral to the tail of the caudate nucleus
AG	Uncinate fasciculus	Connecting amygdala/medial temporal structures and medial prefrontal regions
LG	cingulate segment of the cingulum	Connecting frontal, parietal, and occipital structures
LG	hippocampal segment of the cingulum	Connecting mesial temporal structures
LG	Body of the fornix	Containing fibers directly efferent from the hippocampus

Abbreviations: AG, associative group; LG, limbic group; MSG, motor-sensory group; PyT, pyramidal tract.

lateralization, the AUC of each Z-score was calculated to forecast the left and right sides.

Data availability

The data that support the findings of this study are available from the corresponding author, upon reasonable request.

Results

Patient population

Temporal semiologies, including abdominal aura, absence seizure, and automatism were observed in all 30 HS

patients. All patients were lateralized, either via pathological results or seizure freedom after treatment (Table 1).

Quantified DSI scalar in healthy participants

First, the QA values from the local HC dataset were examined according to fiber group. The distribution of PCs with different axonal diameters is shown in Figure 2A. The mean QA value of different participants in the motor-sensory group was highest (QA: 0.192), followed by the associative (QA: 0.156) and limbic (QA: 0.143) groups; these differences were significant (ANOVA: $F = 27.514$, $p < 0.001$; Bonferroni corrected required p -value of 0.017: $p < 0.001$ within associative and motor-sensory groups; $p < 0.001$ within limbic and motor-sensory groups; $p = 0.166$ within associative and limbic groups; Fig. 2B).

When comparing the neuronal diameter/density of different layers in Von Economo-Koskinas atlas to the average QA values of the corresponding labels in HCP-1021 template, layer IIIc parameters (Tables S2 and S3) were found to have the highest and consistent positive r value of the cell size (Spearman correlation, $r = 0.529$, $p = 0.035$), whereas negative r of the cell density ($r = -0.678$, $p = 0.011$) with the QA values (Fig. 2C).

Quantified DSI scalar study in patients with HS

Compared with HCs, changes in QA values were observed in both left and right HS groups. Notably, lateralization was observed at the cingulum hippocampal segments (Chs), as there appeared to be an ipsilateral decrease in QA value at group level among the left or right HS patients. The mean QA value of Chs decreased on the left side (left HS: 0.132; HC: 0.148; $p < 0.05$) in 19 left HS patients. A decrease in the mean QA value of Chs on the right side (right HS: 0.128; HC: 0.144; $p < 0.05$) was observed in 11 right HS patients. Accordingly, selective loss of pyramidal neurons in HS patients were observed among the affected side of these patients in HE staining and NeuN immunohistochemistry. Additionally, nonselective decline of QA values was observed in the entire fornix (Fig. 3).

The QA distribution in HS patients was similar to that in HCs, specifically, the motor-sensory group was prominently higher than associative and limbic groups (Fig. 3). Regarding the effect of HS on the global white matter bundles extra-temporal lobe in patients, significant changes ($p = 0.005$) were only identified in the left associative group among patients with left HS, which were lower than the QA of the HCs. Whereas all other fiber groups (all the motor-sensory groups and the other

associative groups) were not in statistical significance relative to HCs. Combining the average QA value of the same white matter region across different HCs into a 1 by 48 vector indicating the centroid, the Euclidean distance of the QA values in right HS (0.1019) to the centroid was only 88.53% of the left HS (0.1151), indicating that left HS-induced greater pathological change compared with right HS. Notably, in patients with unfavorable seizure outcomes (PT003, PT005, PT009, PT015, and PT024), the QA values of the extra-temporal white matters decreased below this centroid obviously (Fig. 3E).

Clinical implications of QA values in HS patients: A diagnostic test

Based on the mean and standard of AI in HCs, Z-transformation was performed on the AI of QA values in individual patients. In patients with left HS, a negative Z-score (right-side dominant in relative to the HCs) was observed at the Chs; conversely, in patients with right HS, a positive Z-score (left-side dominant in relative to the HCs) was observed. Z-transformed AI of Chs between left and right HS patients was statistically significant ($p < 0.001$). Both left and right HS exhibited a negative Z-score in the anterior limb of the internal capsule (Fig. 4A).

To evaluate the effect of the AI Z-score when forecasting HS laterality, we plotted the ROC curve and calculated the AUC using the AI Z-scores (zAI) of each white matter region. Age and zAI are uncorrelated (Pearson $r = 0.18$) and independent ($P(\text{age} < 31) = 50\%$, $P(\text{zAI} < -0.4) = 50\%$, and $P(\text{age} < 31, \text{zAI} < -0.4) = 8/30 = 27\%$). The HS affected side was the label to be predicted. The Chs possessed the most notable AUC value, which was 0.957. The best diagnostic performance occurred at Z-transformed AI threshold of -0.027 (sensitivity: 0.909, specificity: 0.895), and the Chs exhibited the highest diagnostic value among the white matter fibers (Fig. 4B).

Discussion

In this study, we explored the value of QA in revealing the tissue properties, and further tested its accuracy in seizure localization. In healthy participants, we observed a negative correlation between QA value and density, and a positive correlation between QA value and cell diameter. Regarding patients with HS, PCs loss and chronic fibrillary gliosis were the typical pathological change,²⁷ and QA values were decreased. Subsequent prediction of HS using the Z-transformed AIs of the QA showed an overall favorable accuracy in the diagnostic test.

QA values among the motor-sensory, associative, and limbic groups were unequally distributed in the present

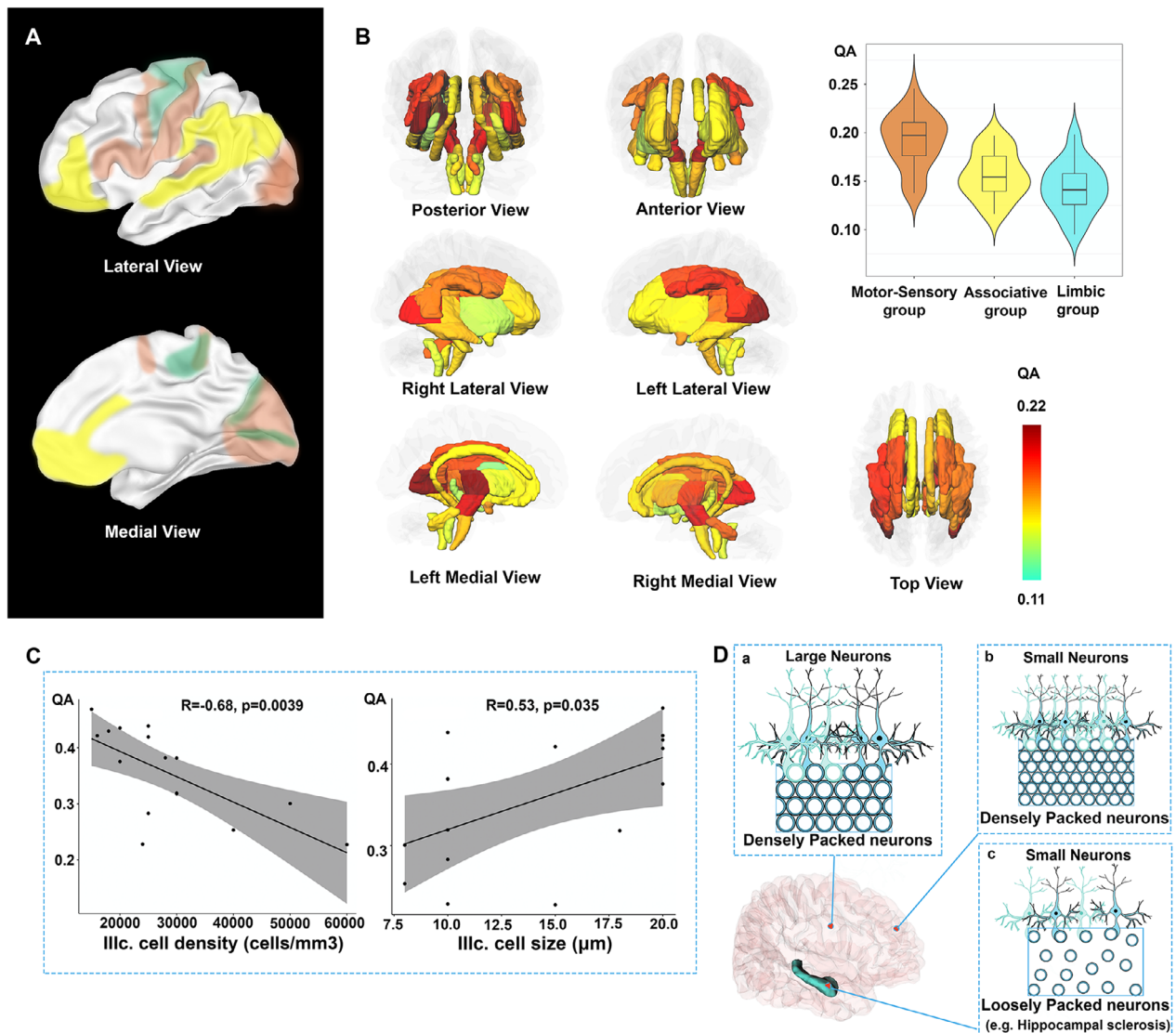


Figure 2. PC content distribution and normal QA distribution. (A) PC content distribution depicting the cellular structure of the human cerebral cortex (Von Economo, C., 2009). Orange: areas consisting of giant PCs in layer III; Green: the sporadic presence of giant cells in layer V; Yellow: areas containing small PCs in layer III. (B) QA map in various views based on 30 healthy participants. Colors close to red and blue represent high and low QA values, respectively. Violin plot of mean QA values of different participants in the motor-sensory (QA: 0.192), associative (QA: 0.156), and limbic (QA: 0.143) group. The QA values decreased in order of the motor-sensory (QA: 0.192), associative (QA: 0.156), and limbic (QA: 0.143) group. (C) The diameters of the cells in layer IIIc were in a positive correlation with the QA values. The density of the cells in layer IIIc was in a negative correlation with the QA values. (D) Schematic picture illustrating different packing paradigm of the cells. According to the Von Economo atlas, the neurons typically account for most of the normal neocortex tissue, and they are packed densely. Thus, in given limited tissue space, the areas with larger neurons (a.) were consistently distributed with less neuronal density, while smaller neurons (b.) were present in a reverse relationship and under pathological state (c.), for example, hippocampal sclerosis, the loss of the pyramidal neurons would happen. QA = quantitative anisotropy, PC = pyramidal cell.

study. In M1 and S1, where the distribution of giant PCs was reported,¹² the QA value was the highest. In areas of the associative group and limbic group with minor to moderate PCs,¹² the QA values were lower. The information (e.g., cell density and diameter) of PCs in the neocortex differ according to location. Von

Economo¹² described the information in terms of density and diameters in a histological atlas. This atlas was recently digitalized into an MRI version,²¹ which made the comparison of neuronal diameter/density with the QA values possible. In further analysis, the increase in cell diameters in layer IIIc was likely associated with an

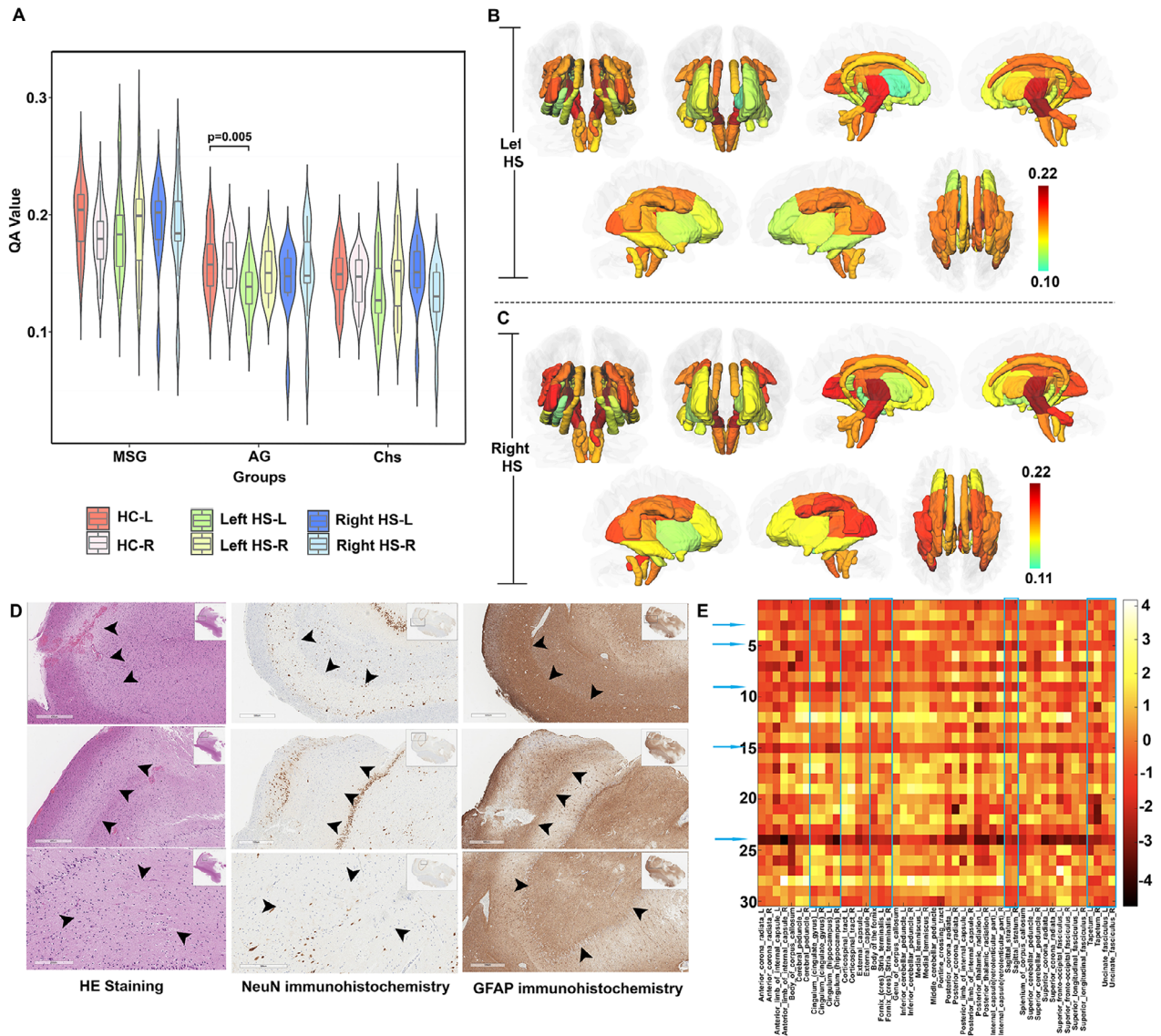


Figure 3. Distribution and variation of QA values among healthy participants and HS patients. (A) Violin plot of QA values in the motor-sensory and associative groups and Chs among healthy participants and left and right HS patients. The Chs QA values were higher on the left side in healthy participants. For left and right HS patients, the Chs QA value decreased on the ipsilateral side of the HS. QA distribution also decreased in the order of the motor-sensory, associative, and limbic groups. A statistically significant change ($p = 0.005$) was only found in the associative group of the left hemisphere in patients with left HS, indicating the potential impact of HS on higher brain function. (B) Mean QA value of each white matter ROI tessellated by color showed the distribution of mean QA values across different fiber tracts in HS patients. The mean Chs QA value in 19 left HS patients decreased on the left side ($p < 0.05$); (C) The decrease in QA value on the right side ($p < 0.05$) was observed according to averaged data of 11 right HS patients; (D) HE staining and NeuN immunohistochemistry showed the loss of pyramidal neurons in hippocampus CA1, CA3 and CA4 regions and granule cell dispersion. GFAP immunohistochemistry showed that astrocyte proliferation in hippocampus CA1, CA3, and CA4 regions; (E) QA's z-values compared with healthy controls (48 white matter ROIs by 30 patients). Temporal lobe-related fibers were highlighted in the blue boxes. Blue arrows indicated patients with unfavorable seizure outcomes (Engel II: PT009, PT024; Engel III: PT003, PT005, PT015). Of note, the decreased QA expanded to extra-temporal white matters in patients who were not seizure-free. HC, healthy controls; HS, hippocampal sclerosis; QA, quantitative anisotropy; MSG, motor-sensory group; AG, associative group; Chs, hippocampal segment of the cingulum.

increase in QA values within the white matter at the subcortical boundary.

Projections of layer IIIc neurons mostly constitute the corpus callosum and the cortico-thalamus fibers.^{28–30}

Thus, these projections mainly account for intra-skull connections, while layer V projections tend to constitute motor, sensory, visual, or auditory fibers that exit the skull.^{28,31} As we observed the white matter QA at the

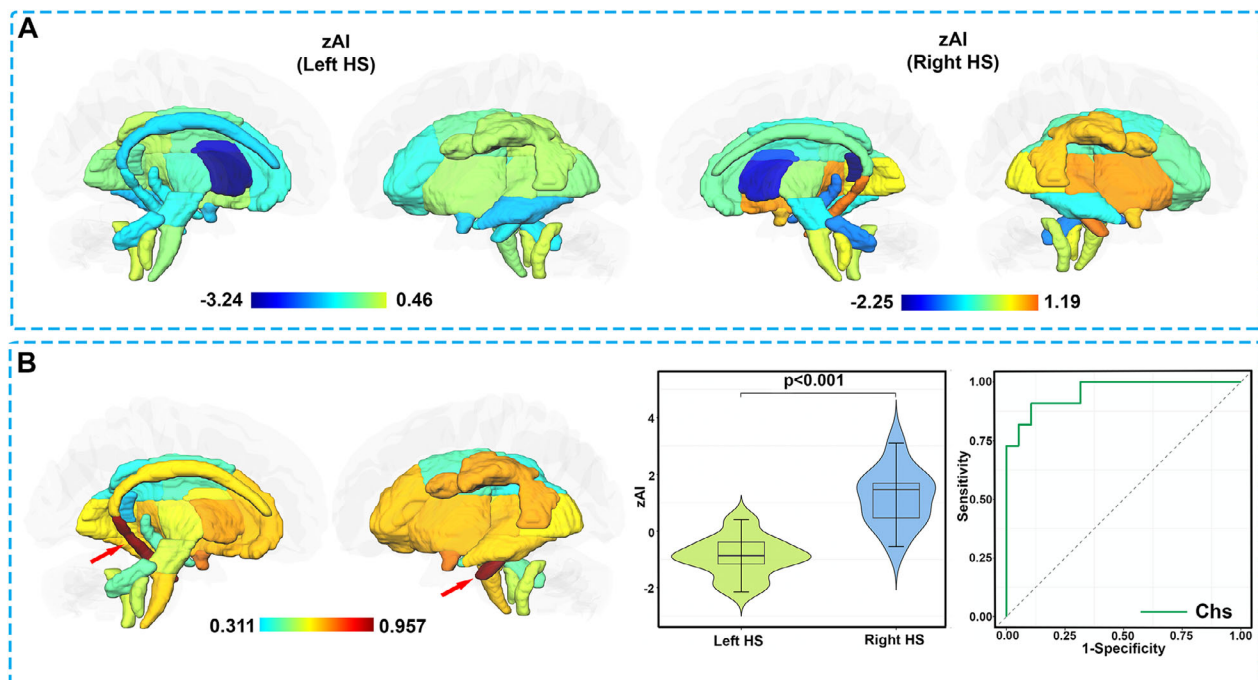


Figure 4. Diagnostic performance of the Z-transformed asymmetry index for the lateralization of hippocampal sclerosis. (A) In left HS patients, right-side dominance appeared at the Chs, whereas in the right HS patients, the Chs showed left-side dominance. Both left and right HS exhibited right-side dominance in the anterior limb of the internal capsule. (B) Heat ROI map of the AUC suggests the highest AUC located at the Chs. Violin plot of zAI in Chs indicated a significant difference of zAI between the left and right HS ($p < 0.001$). The AUC value of the Chs for the affected side of hippocampal sclerosis was 0.957. The Chs exhibited the best diagnostic performance. HS, hippocampal sclerosis; zAI, Z-transformed asymmetry index; Chs, hippocampal segment of the cingulum.

gray–white matter conjunction, the detection of intracranial projections might have been more feasible. Thus, we detected a closer association between the QA and layer IIIc in this study. These observations indicate that evaluating the PCs in the cortices via QA quantification might be justifiable.

Albeit not statistically significant, we observed higher QA values on the left Chs in HCs. Previous studies using diffusion tensor imaging frequently reported that the fractional anisotropy of cingulum tended to be higher on the left side of healthy participants.^{32–34} Highley et al. reported similar findings: the sizes of cells in the left hippocampi of healthy brains tended to be larger,¹⁵ although this cellular asymmetry was not statistically significant. We observed that patients with HS had a significant decrease in QA values at the Chs of the affected side. This might be closely related to the status of the PCs, as HS manifests as a selective loss of pyramidal neurons.¹⁷ As aforementioned, the tracts' QA values may differ between left and right in humans; thus, filtering the AI of HCs using Z-transformation is more justified to evaluate the content of the PCs in epilepsy patients, and the AI Z-scores of the Chs were observed to have a high AUC value to the lateralization of the sclerosed hippocampus.

Previous studies have focused on lateralizing the HS with the diffusion scalars of hippocampal gray matter^{35,36} instead of the Chs. Recent studies reported that FA of the Chs was a sensitive measure for mild cognitive impairment, Alzheimer's disease, and aging.^{37,38} Using a diagnostic test, the present study indicated that QA values of the Chs could also be recognized as a sensitive measure for HS.

Based on the discussions above, we got an initial perception that QA is associated with the tissue properties of different subregions. For example, in a healthy brain where neurons are routinely densely packed,¹² QA would be higher in tissue with low neuronal density and large cell diameters. While in a pathological state that causes PC loss, these cells become loosely packed, and the QA would decrease (Fig. 2D).

Regarding QA changes besides the mesial temporal structures, according to quantitative analysis, the decline in QA of the left hemisphere associative group was found to be statistically significant in left HS patients; conversely, right HS did not cause evident changes to areas external to the mesial temporal lobe. As the associative group is typically involved with higher brain functions, these observations indicated that left HS is more likely to

impact higher brain function than right HS.^{39,40} Furthermore, according to previous literature of fMRI, the left HS would have a much dominant impact to higher brain functions, such as memory, and language.^{41,42,43} This is in line with our observations. Besides, a vast decrease of the QA values mainly appeared in patients with unfavorable seizure outcomes, indicating that low QA values in areas outside the anterior temporal lobe may be a predictor of seizure recurrence.

Although the QA values were validated with tissue properties, limitations still exist, as the cellular data were from the literature instead of histological experiments. Moreover, the sample size of the series was limited. Only 11 cases of right HS were enrolled; thus, further studies with larger sample sizes are needed in the future. Furthermore, as the present study focused on the diffusion scalars, procedures involved with fiber tracking, such as U-fiber quantification, would be investigated in future research. Additionally, the main objective of this study was to preliminarily describe the association between the QA and tissue properties, and further explore its clinical application in TLE patients; Thus, future studies are needed to quantify QA usage in patients with neocortical epilepsy.

In summary, based on the DSI data of 30 healthy participants and the HCP-1021 template, we preliminarily found the QA values might be potential to reveal the tissue properties of different brain areas in HCs. Further, using a diagnostic test, we indicated that the QA value of the Chs could be a reliable measure for the lateralization of HS in patients with the epileptic disease. Future studies on the QA scalar might provide an in-depth and noninvasive approaches to various seizures' localizations.

Acknowledgement

This project was supported by Beijing Municipal Administration of Hospitals' Ascent Plan (DFL20180802), the National Natural Science Foundation of China (grant numbers 81871009, 81801288, 82030037, 81790652), Huizhi Ascent Project of Xuanwu Hospital (HZ2021ZCLJ005), and Beijing Hospitals Authority Youth Program (QML20190805). Data were provided in part by the Human Connectome Project, WU-Minn Consortium (Principal Investigators: David Van Essen and Kamil Ugurbil; 1U54MH091657) funded by the 16 NIH Institutes and Centers that support the NIH Blueprint for Neuroscience Research; and by the McDonnell Center for Systems Neuroscience at Washington University.

Author Contributions

Zhen-Ming Wang: Conceptualization, Methodology, Validation, Formal analysis, Writing - original draft. Peng-Hu

Wei: Conceptualization, Methodology, Software, Formal analysis. Miao Zhang: Methodology, Investigation (Radiologist). Chunxue Wu: Investigation (Radiologist). Yi Shan: Methodology. Fang-Cheng Yeh: Supervision. Yongzhi Shan: Investigation (Neurosurgeon). Jie Lu: Conceptualization, Writing - review & editing, Supervision. All coauthors have seen and agreed with the contents of the manuscript.

Conflict of Interest

None.

References

- Schmidt D, Sillanpää M. Evidence-based review on the natural history of the epilepsies. *Curr Opin Neurol*. 2012;25(2):159-163.
- Nicoletti A, Sofia V, Vitale G, et al. Natural history and mortality of chronic epilepsy in an untreated population of rural Bolivia: a follow-up after 10 years. *Epilepsia*. 2009;50(10):2199-2206.
- Pfisterer U, Petukhov V, Demharter S, et al. Identification of epilepsy-associated neuronal subtypes and gene expression underlying epileptogenesis. *Nat Commun*. 2020;11(1):5038.
- Patel DC, Tewari BP, Chaunsali L, Sontheimer H. Neuron-glia interactions in the pathophysiology of epilepsy. *Nat Rev Neurosci*. 2019;20(5):282-297.
- Von Oertzen J, Urbach H, Jungbluth S, et al. Standard magnetic resonance imaging is inadequate for patients with refractory focal epilepsy. *J Neurol Neurosurg Psychiatry*. 2002;73(6):643-647.
- Ji GJ, Zhang Z, Xu Q, Zang YF, Liao W, Lu G. Generalized tonic-clonic seizures: aberrant interhemispheric functional and anatomical connectivity. *Radiology*. 2014;271(3):839-847.
- Farquharson S, Tournier JD, Calamante F, et al. Periventricular nodular heterotopia: detection of abnormal microanatomic fiber structures with whole-brain diffusion MR imaging tractography. *Radiology*. 2016;281(3):896-906.
- Douglas RJ, Martin KA. Neuronal circuits of the neocortex. *Annu Rev Neurosci*. 2004;27:419-451.
- Gilbert CD, Li W. Top-down influences on visual processing. *Nat Rev Neurosci*. 2013;14(5):350-363.
- Reid RC, Alonso JM. The processing and encoding of information in the visual cortex. *Curr Opin Neurobiol*. 1996;6(4):475-480.
- Senzai Y, Fernandez-Ruiz A, Buzsáki G. Layer-specific physiological features and interlaminar interactions in the primary visual cortex of the mouse. *Neuron*. 2019;101(3):500-13.e5.
- Von Economo C. Cellular structure of the human cerebral cortex. Karger Medical and Scientific Publishers; 2009.

13. Kushchayev SV, Moskalenko VF, Wiener PC, et al. The discovery of the pyramidal neurons: Vladimir Betz and a new era of neuroscience. *Brain*. 2012;135(Pt 1):285-300.
14. Wagstyl K, Larocque S, Cucurull G, et al. BigBrain 3D atlas of cortical layers: cortical and laminar thickness gradients diverge in sensory and motor cortices. *PLoS Biol*. 2020;18(4):e3000678.
15. Highley JR, Walker MA, McDonald B, Crow TJ, Esiri MM. Size of hippocampal pyramidal neurons in schizophrenia. *Br J Psychiatry*. 2003;183:414-417.
16. Hevner RF. From radial glia to pyramidal-projection neuron: transcription factor cascades in cerebral cortex development. *Mol Neurobiol*. 2006;33(1):33-50.
17. DeGiorgio CM, Tomiyasu U, Gott PS, Treiman DM. Hippocampal pyramidal cell loss in human status epilepticus. *Epilepsia*. 1992;33(1):23-27.
18. Yeh FC, Wedeen VJ, Tseng WY. Generalized q-sampling imaging. *IEEE Trans Med Imaging*. 2010;29(9):1626-1635.
19. Gok B, Jallo G, Hayeri R, Wahl R, Aygun N. The evaluation of FDG-PET imaging for epileptogenic focus localization in patients with MRI positive and MRI negative temporal lobe epilepsy. *Neuroradiology*. 2013;55(5):541-550.
20. Wang YH, Wang ZM, Wei PH, et al. Lateralizing the affected side of hippocampal sclerosis with quantitative high angular resolution diffusion scalars: a preliminary approach validated by diffusion spectrum imaging. *Ann Transl Med*. 2021;9(4):297.
21. Scholtens LH, de Reus MA, de Lange SC, Schmidt R, van den Heuvel MP. An MRI Von Economo - Koskinas atlas. *Neuroimage*. 2018;15(170):249-256.
22. Wang ZM, Wei PH, Shan Y, et al. Identifying and characterizing projections from the subthalamic nucleus to the cerebellum in humans. *Neuroimage*. 2020;15(210):116573.
23. Mtui E, Gruener G, Dockery P. Fitzgerald's Clinical Neuroanatomy and Neuroscience E-Book. Elsevier; 2020.
24. Schmahmann JD, Schmahmann J, Pandya D. Fiber pathways of the brain. OUP USA; 2009.
25. Honnedevasthana Arun A, Connelly A, Smith RE, Calamante F. Characterisation of white matter asymmetries in the healthy human brain using diffusion MRI fixel-based analysis. *Neuroimage*. 2021;15(225):117505.
26. Büchel C, Raedler T, Sommer M, Sach M, Weiller C, Koch MA. White matter asymmetry in the human brain: a diffusion tensor MRI study. *Cereb Cortex*. 2004;14(9):945-951.
27. Malmgren K, Thom M. Hippocampal sclerosis--origins and imaging. *Epilepsia*. 2012;53(Suppl 4):19-33.
28. Anderson CT, Sheets PL, Kiritani T, Shepherd GM. Sublayer-specific microcircuits of corticospinal and corticostriatal neurons in motor cortex. *Nat Neurosci*. 2010;13(6):739-744.
29. Broser P, Grinevich V, Osten P, Sakmann B, Wallace DJ. Critical period plasticity of axonal arbors of layer 2/3 pyramidal neurons in rat somatosensory cortex: layer-specific reduction of projections into deprived cortical columns. *Cereb Cortex*. 2008;18(7):1588-1603.
30. Kaneko T, Cho R, Li Y, Nomura S, Mizuno N. Predominant information transfer from layer III pyramidal neurons to corticospinal neurons. *J Comp Neurol*. 2000;423(1):52-65.
31. Hooks BM, Papale AE, Paletzki RF, et al. Topographic precision in sensory and motor corticostriatal projections varies across cell type and cortical area. *Nat Commun*. 2018;9(1):3549.
32. Gong G, Jiang T, Zhu C, et al. Asymmetry analysis of cingulum based on scale-invariant parameterization by diffusion tensor imaging. *Hum Brain Mapp*. 2005;24(2):92-98.
33. Thiebaut de Schotten M, Ffytche DH, Bizzi A, et al. Atlas location, asymmetry and inter-subject variability of white matter tracts in the human brain with MR diffusion tractography. *Neuroimage*. 2011;54(1):49-59.
34. Takao H, Hayashi N, Ohtomo K. White matter microstructure asymmetry: effects of volume asymmetry on fractional anisotropy asymmetry. *Neuroscience*. 2013;12(231):1-12.
35. Liu M, Bernhardt BC, Hong SJ, Caldairou B, Bernasconi A, Bernasconi N. The superficial white matter in temporal lobe epilepsy: a key link between structural and functional network disruptions. *Brain*. 2016;139(Pt 9):2431-2440.
36. Chang YA, Marshall A, Bahrami N, et al. Differential sensitivity of structural, diffusion, and resting-state functional MRI for detecting brain alterations and verbal memory impairment in temporal lobe epilepsy. *Epilepsia*. 2019;60(5):935-947.
37. Nir TM, Jahanshad N, Villalon-Reina JE, et al. Effectiveness of regional DTI measures in distinguishing Alzheimer's disease, MCI, and normal aging. *Neuroimage Clin*. 2013;3:180-195.
38. Ezzati A, Katz MJ, Lipton ML, Zimmerman ME, Lipton RB. Hippocampal volume and cingulum bundle fractional anisotropy are independently associated with verbal memory in older adults. *Brain Imaging Behav*. 2016;10(3):652-659.
39. Saling MM, Berkovic SF, O'Shea MF, Kalnins RM, Darby DG, Bladin PF. Lateralization of verbal memory and unilateral hippocampal sclerosis: evidence of task-specific effects. *J Clin Exp Neuropsychol*. 1993;15(4):608-618.
40. Hermann BP, Seidenberg M, Schoenfeld J, Davies K. Neuropsychological characteristics of the syndrome of mesial temporal lobe epilepsy. *Arch Neurol*. 1997;54(4):369-376.

41. Kucukboyaci NE, Kemmotsu N, Cheng CE, et al. Functional connectivity of the hippocampus in temporal lobe epilepsy: feasibility of a task-regressed seed-based approach. *Brain Connect.* 2013;3(5):464-474.
42. Nenning KH, Fösleitner O, Schwartz E, et al. The impact of hippocampal impairment on task-positive and task-negative language networks in temporal lobe epilepsy. *Clin Neurophysiol.* 2021;132(2):404-411.
43. Roger E, Pichat C, Torlay L, et al. Hubs disruption in mesial temporal lobe epilepsy. A resting-state fMRI study on a language-and-memory network. *Hum Brain Mapp.* 2020;41(3):779-796.

Supporting Information

Additional supporting information may be found online in the Supporting Information section at the end of the article.

Table S1 Clinical features of the patients.

Table S2 Cell size (μm) in areas from Von Economo-Koskinas atlas.

Table S3 Cell density (cells/mm³) in areas from Von Economo-Koskinas atlas.